Effects of oxygen partial pressure on optical absorption edge and UV emission energy of ZnO films

Ruijin Hong (洪瑞金)[1,2], Jianda Shao (邵建达)[1], Hongbo He (贺洪波)[1], and Zhengxiu Fan (范正修)[1]

[1] *Research and Development Center for Optical Thin Film Coatings, Shanghai Institute of Optics and Fine Mechanics, Chinese Academy of Sciences, Shanghai 201800*

[2] *Graduate School of Chinese Academy of Sciences, Beijing 100864*

Received September 15, 2004

The optical absorption edge and ultraviolet (UV) emission energy of ZnO films deposited by direct current (DC) reactive magnetron sputtering at room temperature have been investigated. With the oxygen ratio increasing, the structure of films changes from zinc and zinc oxide coexisting phase to single-phase ZnO and finally to the highly (002) orientation. Both the grain size and the stress of ZnO film vary with the oxygen partial pressure. Upon increasing the oxygen partial pressure in the growing ambient, the visible emission in the room-temperature photoluminescence spectra was suppressed without sacrificing the band-edge emission intensity in the ultraviolet region. The peaks of photoluminescence spectra were located at 3.06—3.15 eV. From optical transmittance spectra of ZnO films, the optical band gap edge was observed to shift towards shorter wavelength with the increase of oxygen partial pressure.

OCIS codes: 310.0310, 300.6470, 310.6860, 170.6280.

ZnO, with a band-gap of 3.37 eV and a large exciton binding energy (about 60 meV) at room temperature, is a promising material for optoelectronic devices, field-emission displays, and gas sensors. Recently, the interest in short wavelength display device is on the increase. In this regard, ZnO is a promising material[1−6].

High quality ZnO films have been prepared by many methods such as sputtering[7], reactive thermal and electron-beam evaporation[8], pulse laser deposition[9], chemical vapor deposition[10], oxidation of metallic Zn[11], and molecular beam epitaxy[12]. Among all, magnetron sputtering is characterized by several advantages, such as low substrate temperature (down to room temperature), good adhesion of films on substrates, very good thickness uniformity and high density of the films, and directive deposition from elemental (metallic) targets by reactive sputtering in rare/reactive gas mixtures[13].

The fundamental absorption refers to band-to-band or to exciton transitions, i.e., to the excitation of an electron from the valence band to the conduction band. The fundamental absorption, which manifests itself by a rapid rise in absorption, can be used to determine the energy gap of the semiconductor. A study of the photoluminescence (PL) structure of ZnO is interesting because it can provide valuable information on the quality and purity of the materials. The PL spectrum of ZnO is normally composed of two parts: excitonic near band edge emission with energy around the band gap of ZnO and defect related deep level emission in the visible range. Stoichiometric ZnO thin films usually show strong ultraviolet (UV) luminescence. The UV emission is due to excitonic related recombination[14]. The emission properties of ZnO films are strongly dependent on the growth condition.

Although oxygen partial pressure effects on ZnO optical properties have been researched[15,16], the influence of oxygen partial pressure on the non-annealed ZnO optical properties has been seldom studied. In this letter, we report the study on the optical absorption edge and UV emission energy of the as grown ZnO films sputtered at room temperature without annealing.

ZnO films were grown by direct current (DC) planar magnetron sputtering using 8.6 cm-in-diameter Zn target (99.999%) on Si (100) and fused silica at room temperature. The substrates were rinsed in acetone, ethanol and distilled water sequentially, and dried by nitrogen before being loaded into the growth chamber. High purity argon and oxygen were used as the sputtering and reactive gases respectively. The chamber was pumped to a base pressure of 1×10^{-3} Pa before deposition. Film growth was carried out in the growth ambient with $O_2/Ar+O_2$ ratios ranging from 0.30 to 0.80 at a constant working pressure of 0.15 Pa.

The crystal structure of the films was characterized by X-ray diffraction (XRD) using a Rigaku D/Max-B system, with Cu K_α adiation ($\lambda = 0.15408$ nm). Biaxial film stress σ and the average crystallite size D were evaluated from XRD $\theta - 2\theta$ scans. PL spectra of the films were measured by fluorescence spectrophotometer (JASCO FP-6500) with wavelength range of 350—750 nm, the excitation light was the 325 nm line of xenon lamp. The optical transmittance and absorption of the films were measured with UV-VIS-NIR double beam spectrophotometer (Perkin-Elmer, USA). All measurements were carried out at room temperature.

Figure 1 shows the XRD spectra of the ZnO films prepared by DC reactive magnetron sputtering under various oxygen partial pressures at room temperature. It can be observed that the phase and composition of the films grown at room temperature strongly depend on oxygen partial pressure. The films have both zinc and zinc oxide peaks when the oxygen concentration is less than 40%, the dominant phase of the films is metal zinc. Single-phase ZnO films can be prepared at room temperature when the oxygen concentration is above 40%, when the oxygen partial pressure is around 40%, the film is

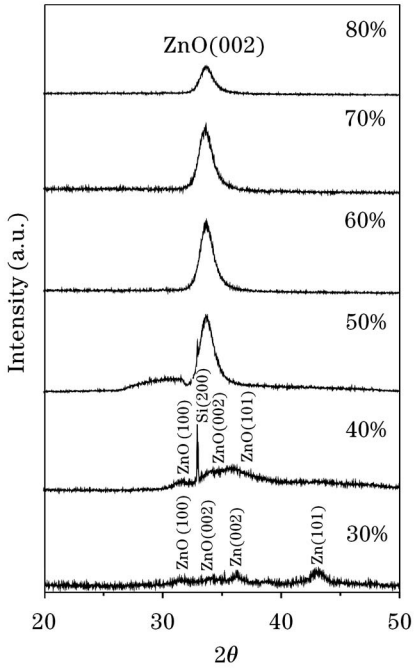

Fig. 1. XRD patterns of ZnO films grown at room temperature with various oxygen partial pressures.

polycrystalline with a hexagonal crystal structure. With the increase of oxygen partial pressure, the around 34° diffraction peak of the films was observed corresponding to the (002) orientation of ZnO. The surface energy density of the (002) orientation is the lowest in the ZnO crystal. Grains with the lower surface energy will become larger as the film grows. Then, the growth orientation develops into one crystallographic direction of the lowest surface energy. This means that the (002) textured film must form in an effective equilibrium state where enough surface mobility is given to impinging atoms under a certain deposition condition[17]. It is seen that the (002) peak intensity increases with the increase of oxygen partial pressure up to 50%, thereafter decreases when the oxygen partial pressure further increases. The full width at half maximum (FWHM) for (002) orientation decreases with the increase of oxygen partial pressure.

The microstructure and stresses in a vacuum-deposited coating film are sensitive to the deposition conditions. Compared with zinc oxide powders, all the films formed in our experiment exhibit discrepancy in d-value (d is interplanar spacing), which was due to the variation of residual stress developed in the films. From the integral width and peak position of the (002) peak, grain size and stress in the films have been calculated (see Fig. 2). It shows that the grain size and the film stress are dependent on the oxygen partial pressure. The average grain sizes in the films are ranged from 5.9 to 6.7 nm, and the film stresses are from 4.39 to 4.93 GPa. The average grain size in the films can be estimated by the Scherrer formula using the FWHM value of the XRD diffraction peaks. The Scherrer formula[18] is

$$D = \frac{0.9\lambda}{B\cos\theta}, \tag{1}$$

where D, λ, θ, and B are the mean grain size, the X-ray wavelength of 0.154 nm, Bragg diffraction angle, and FWHM of the diffraction peak of the (002) direction at around 34 (2θ) for ZnO films, respectively. The calculation of the film stress is based on the biaxial strain model. The strain $\varepsilon = (c_{\rm film} - c_{\rm bulk}/c_{\rm bulk})$ in direction of the c axis, i.e., perpendicular to the substrate surface was measured by XRD, where $c_{\rm film}$ and $c_{\rm bulk}$ are the lattice parameter of film and the strain-free lattice parameter of ZnO powder sample, respectively. The lattice constant c for hexagonal close packed ZnO is equal to twice the interplanar spacing d of the basal planes, measured from the position of the (002) peak using Bragg equation. To derive the film stress $\sigma_{\rm film}$ parallel to the film surface, the following formula has been used, which is valid for a hexagonal lattice

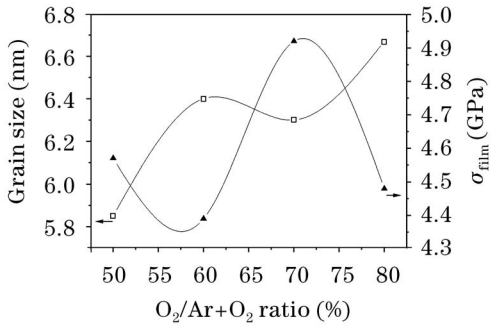

Fig. 2. Variation of grain size, and mechanical stress $\sigma_{\rm film}$ of ZnO films with oxygen partial pressure.

$$\sigma_{\rm film}^{\rm XRD} = \frac{2c_{13}^2 - c_{33}(c_{11}+c_{12})}{2c_{13}} \cdot \frac{c_{\rm film} - c_{\rm bulk}}{c_{\rm bulk}}. \tag{2}$$

For the elastic constants c_{ij}, data of single crystalline ZnO have been used: c_{11} = 208.8, c_{33} = 213.8, c_{12} = 119.7, c_{13} = 104.2 GPa[19]. This yields the following numerical relation for the stress derived from XRD: $\sigma_{\rm film} = 233\varepsilon$ [GPa].

PL emission is one of the most important properties of ZnO. Figure 3 presents room temperature PL spectra of the ZnO films prepared under different oxygen partial pressure. The shape of all the spectra, being similar to those reported by Ref. [20], is featured by a strong emission near UV peak and a weak defect-related deep level emission in visible region. The origin of the observed near-UV lines was identified in terms of bound exciton complexes and the phonon replicas due to emission of a single optical phonon or two phonons. All the PL peaks showed a Stokes shift, i.e., the peak energies were lower than the absorption energy. The UV emission peaks vary with the increase of oxygen partial pressure, peaking around 393—405 nm. Also from the spectra, it is noticeable that the relative intensity of the visible emission peak abruptly decreases as the oxygen partial pressure increases, depending markedly on the growth ambient.

It is well known that the light emission intensity was determined by the radiative and nonradiative transition. The luminescence efficiency of the light emission can be described by the following formula[21]

$$\eta = \frac{I_{\rm R}}{I_{\rm R} + I_{\rm NR}}, \tag{3}$$

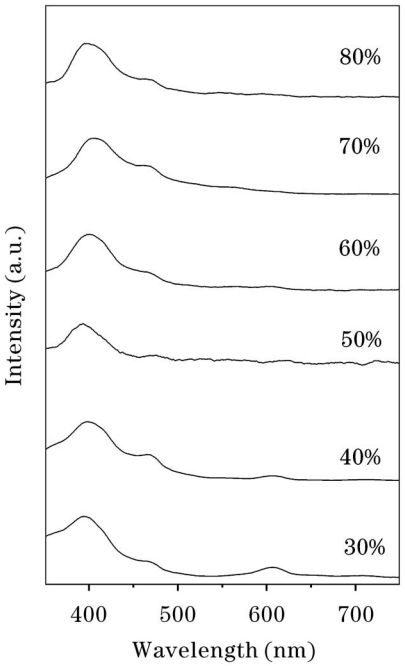

Fig. 3. Room temperature photoluminescence spectra of ZnO films deposited under different oxygen partial pressures.

where η is luminescence efficiency, I_{R} and I_{NR} are radiative and nonradiative transition probabilities, respectively. In the case of ZnO, the nonradiative transition is induced by crystal imperfections, such as point defects, dislocations and grain boundaries. The radiative transition is composed of two parts as indicated above, near band edge excitonic related UV emission and deep level emission. Deep level emission is determined by the concentration of the corresponding defects. So there are two kinds of imperfections in ZnO, one induces nonradiative transition and the other induces deep level emission. For the as-grown ZnO films prepared by DC reactive sputtering without annealing, the chemical component was nonstoichiometric, and usually consisted excess Zn atoms. Therefore, many lattice defects and surface defects were contained in the as-grown ZnO films. These defects produced various nonradiative centers and reduced light emission from the ZnO. With the increase of oxygen partial pressure, the defects in ZnO thin films decrease. Accordingly, the intensity of visible emission decreases. It has been reported that the PL emission characteristics of ZnO films are strongly dependent on both the crystal quality of the film and the film stoichiometry[22]. For the ZnO thin films prepared under various oxygen partial pressures at room temperature. No obvious crystal changes were observed. According to Fig. 3, the luminescence property was mainly dependent on the stoichiometry.

The film stoichiometry was indirectly evaluated by observing the optical transmittance spectra. With the oxygen concentration increasing, the plasma edge, which results from the onset of fundamental absorption, is observed to shift towards shorter wavelengths. All the films grown under the oxygen concentration above 40% exhibit high transmittance in the visible range. The lower transmittance of the film grown under an oxygen-deficient condition can originate from the defect electronic states

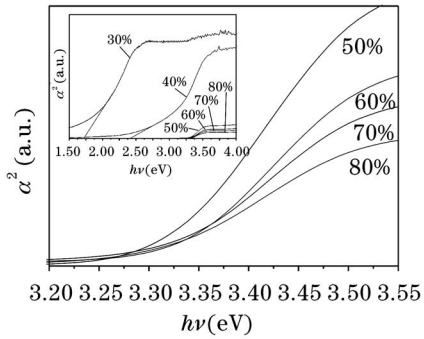

Fig. 4. α^2 versus $h\nu$ curves for the optical band gap determination in ZnO films grown under various oxygen partial pressures.

within the band gap associated with oxygen vacancies and interstitial Zn atoms[16]. Thus, this improvement of the optical transmittance under the oxygen-rich condition is evaluated as a clear indicator that the film stoichiometry is gradually improved as the $O_2/Ar+O_2$ ratio increased. We also found the phenomena of absorption edge shifts from the plots of optical density versus photon energy.

In order to calculate the band gap energies of the thin films, we assumed the absorption coefficient $\alpha \propto \log(\frac{1}{T})$ corresponding to the direct band gap of wurtzite structure ZnO. We have made a plot of $[\alpha(h\nu)]^2$ against the photon energy $h\nu$. Figure 4 shows the α^2 versus photon energy curves of ZnO films deposited at various oxygen partial pressures, where α represents the absorption coefficient and $h\nu$ hoton energy. The ZnO films have optical band gap energy of 1.72, 2.42, 3.33, 3.34, 3.35, and 3.31, which corresponds to the oxygen partial pressure of 30%, 40%, 50%, 60%, 70%, and 80%, respectively.

We have shown that the oxygen partial pressure strongly influences the structure and the optical properties of ZnO films grown by DC reactive magnetron sputtering. XRD results reveal that the as-grown ZnO films have zinc and zinc oxide coexisting phase when the oxygen concentration is low, and the structure of films transforms into single-phase ZnO and then further into the (002) orientation with the oxygen partial pressure increasing. The room temperature PL spectra of the as-grown ZnO films reveal that the violet emission is mainly dependent on the stoichiometry. The varieties of PL peak position in the range of UV are not consistent with those of optical band gap. The optical transmission of ZnO films is also strongly dependent on oxygen concentration. The films exhibit opaque at low oxygen concentration, while transparent for the oxygen concentration more than 40%.

R. Hong's e-mail address is rjhong@mail.siom.ac.cn.

References

1. X. P. Peng, Y. H. Yang, C. A. Song, and Y. Y. Wang, Acta Opt. Sin. (in Chinese) **24,** 1459 (2004).
2. D. J. Chen, K. X. Zhang, B. Shen, Y. Z. Deng, L. Pu, R. Zhang, Y. Shi, and Y. D. Zheng, Acta Opt. Sin. (in Chinese) **24,** 137 (2004).
3. D. C. Look, Mater. Sci. Eng. B **80,** 383 (2001).

4. D. Wiersma, Nature **406,** 132 (2000).
5. P. H. Holloway, T. A. Trottier, B. Abrams, C. Kondoleon, S. L. Jones, J. S. Sebastian, W. J. Thomas, and H. Swart, J. Vac. Sci. Technol. B **17,** 758 (1999).
6. H. Cao, J. Y. Xu, D. Z. Zhang, S.-H. Chang, S. T. Ho, E. W. Seelig, X. Liu, and R. P. H. Chang, Phys. Rev. Lett. **84,** 5584 (2000).
7. K.-K. Kim, J.-H. Song, H.-J. Jung, and W.-K. Choi, J. Appl. Phys. **87,** 3573 (2000).
8. H. Z. Wu, K. M. He, D. J. Qui, and D. M. Huang, J. Cryst. Growth **217,** 131 (2000).
9. S. H. Bae, S. Y. Lee, B. J. Jin, and S. Im, Appl. Surf. Sci. **154,** 458 (2000).
10. S. A. Studenikin, N. Golego, and M. Cocivera, J. Appl. Phys. **84,** 2287 (1998).
11. Y. G. Wang, S. P. Lau, H. W. Lee, S. F. Yu, B. K. Tay, X. H. Zhang, and H. H. Hng, J. Appl. Phys. **94,** 354 (2003).
12. Y. F. Chen, D. Bagnall, and T. F. Yao, Mater. Sci. Eng. B **75,** 190 (2000).
13. K. Ellmer, J. Phys. D: Appl. Phys. **33,** R17 (2000).
14. D. C. Reynolds, D. C. Look, B. Jobai, C. W. Litton, T. C. Collins, W. Harsch, and G. Cantwell, Phys. Rev. B **57,** 12151 (1998).
15. K. Ellmer, F. Kudella, R. Mientus, R. Schieck, and S. Fiechter, Thin Solid Films **247,** 15 (1994).
16. S. H. Jeong, B. S. Kim, and B. T. Lee, Appl. Phys. Lett. **82,** 2625 (2003).
17. N. Fujimura, T. Nishihara, S. Goto, J. Xu, and T. Ito, J. Cryst. Growth **130,** 269 (1993).
18. B. D. Cullity, *Elements of X-Ray Diffractions* (Addition-Wesley, Reading, MA, 1978) p.102.
19. R. Cebulla, R. Wendt, and K. Ellmer, J. Appl. Phys. **83,** 1087 (1998).
20. S. L. Cho, J. Ma, Y. K. Kim, Y. Sun, G. K. L. Wong, and J. B. Ketterson, Appl. Phys. Lett. **75,** 2761 (1999).
21. S. Shionoya and W. M. Yen, *Phosphor Handbook* (Chemical Rubber, Cleveland, 1999).
22. Z. K. Tang, G. K. L. Wong, and P. Yu, Appl. Phys. Lett. **72,** 3270 (1998).